Vol. 71: 139–153, 2016
doi: 10.3354/cr01433

CLIMATE RESEARCH
Clim Res

Published December 28

Atmospheric circulation characteristics favouring extreme precipitation in Turkey

C. J. Lolis[1,*], M. Türkeş[2]

[1]Laboratory of Meteorology, Department of Physics, University of Ioannina, 45110 Ioannina, Greece
[2]Bogazici University Center for Climate Change and Policy Studies, 34342 İstanbul, Turkey

ABSTRACT: The atmospheric circulation characteristics over Europe and the Mediterranean that favour extreme precipitation in Turkey are analysed. In total, 326 extreme precipitation events in Turkey are defined using a criterion involving the upper 1 and 5% percentiles of daily precipitation at 70 meteorological stations for the period 1979 to 2011. The 500 and 1000 hPa standard pressure level geopotential heights, 850 hPa level air temperature and relative humidity, 500 hPa level relative vorticity, 925 hPa level divergence and convective available potential energy obtained from the ERA-Interim data set are examined for the days before, during and after the events. A multivariate statistical approach including factor analysis and k-means cluster analysis is followed, and the events are classified into 7 clusters according to the corresponding atmospheric circulation characteristics. The results show that in most cases, a west to east movement of strong upper air disturbances (mainly troughs with strong gradient toward or over Turkey) and low-pressure systems over the Eastern Mediterranean Basin, particularly south of Turkey, play a significant role for the occurrence of extreme precipitation events. The details referring to the areas of low level convergence, positive vorticity advection, high relative humidity and instability play a dominant role in the spatial and temporal distribution of the events.

KEY WORDS: Turkey · Mediterranean · Extreme precipitation · Atmospheric circulation · Factor analysis · k-means cluster analysis

1. INTRODUCTION

Precipitation is a meteorological and climatological element of great importance because it controls vegetation, agricultural production and water resources, while extreme precipitation may be responsible for floods leading to disasters, to significant infrastructure damage and sometimes to the loss of human lives. The complexity of impacts resulting from extreme precipitation events varies with their spatial coherence, which depends on the atmospheric circulation characteristics and the topography (Parker & Abatzoglou 2016). The atmospheric circulation characteristics that favour extreme precipitation are of considerable interest, taking into account that a high percentage of precipitation extremes is related to cyclonicity. The percentage of cyclone-induced precipitation extremes exceeds 80% over some parts of the globe, including the Mediterranean region (Pfahl & Wernli 2012). In the Mediterranean region, the link between extreme precipitation and atmospheric circulation is important because the Mediterranean basin is located in a sensitive transitional climatic zone between the subtropics and the westerlies, and any possible changes in circulation could significantly affect the frequency and intensity of precipitation extremes. Extreme precipitation in the Mediterranean region and its connection to specific atmospheric processes at various scales have been examined during the last decade with the use of different approaches and techniques. Houssos et al. (2008) found 9 main types of atmospheric circulation

*Corresponding author: chlolis@uoi.gr

favouring extreme precipitation at 3 meteorological stations in Greece using S-mode factor analysis and k-means cluster analysis. Flaounas et al. (2013) retrieved the space-time variability of precipitation as well as its extremes in the Mediterranean region, using both dynamical and statistical downscaling methods over the 1989–2008 period. Nastos et al. (2013) compared and analysed TRMM 3B42 satellite precipitation extremes against the E-OBS project high-resolution gridded precipitation dataset over the Mediterranean region for the period 2000 to 2011, revealing considerable regional differences in precipitation indices between the 2 datasets. Krichak et al. (2014a) examined the relationship between the frequency of extreme precipitation in the Euro-Mediterranean region and the main teleconnection patterns (NAO, AO, EAWR SCAND, and ENSO) using NCEP/NCAR reanalysis data and found statistically significant correlation coefficients. Krichak et al. (2014b) examined the role of humid tropical air export in the formation of cold-season heavy precipitation in the Mediterranean region and its linkage to the multiyear trend in precipitation extremes. They found that the linear trend (1979–2013) of the frequency of humid days is consistent with the recent changes in the precipitation character. Winschall et al. (2014) investigated the significance of intensified evaporation for Northwestern Mediterranean precipitation extremes and found that the convergence from the background moisture reservoir is essential, while anomalously intense surface evaporation is required for the remote sources of the North Atlantic and the European and African land surfaces. Toreti et al. (2015) studied daily precipitation extremes over the Mediterranean region and the associated upper-level atmospheric dynamics, revealing a high spatial variability of extremes over the basin as a whole, changes in temporal variability across the basin and the influence of orographic lifting on the low-level flow. Dayan et al. (2016) discussed the dynamic and thermodynamic processes that favour heavy rainfall over the Eastern and the Western Mediterranean, taking into account published studies on extreme precipitation events.

The Mediterranean type climate zones over the various areas of the world are mainly dominated by subtropical high-pressure cells of dynamical origin (e.g. Azores High Pressure System over the mid-north Atlantic for the 'real' Mediterranean climate zone) during late spring, summer and early fall. During this period of the year, the adiabatic sinking of relatively dry and stable air masses does not generally favour precipitation. Occasional local-scale precipitation events (including showers and thunderstorms) are associated with thermal and orographic factors. In contrast, during mid-late fall, winter and early-mid spring, the polar jet-stream and the associated mid-latitude cyclones (i.e. frontal winter storms) reach into the subtropical Mediterranean climate zones, and the frontal low-pressure systems bring high amounts of rainfall along with snow on the mountains (Lolis et al. 2008, 2012, Türkeş 2010).

The Eastern Mediterranean region comprising Turkey and other coastal countries is characterized mainly by the dry and hot/very hot summer subtropical Mediterranean macroclimate being driven and controlled by an unequivocal seasonal alteration between the mid-latitude and the sub-tropical/tropical pressure and wind systems (circulation patterns) from winter to summer. As a result, there is high seasonal variability in the precipitation regime of the western and southern regions of Turkey (Türkeş 1998, 2010). Consequently, the regions of Turkey characterised by the dry summer subtropical Mediterranean climate (e.g. İzmir, Aydın, Antalya, Mersin, etc.) receive more than half of their yearly precipitation amounts during winter, late autumn and early spring months (Türkeş 2003, Türkeş et al. 2016).

The precipitation climatology, the drought events and their spatial distribution, and the long-term variability, trends and changes in precipitation series over Turkey have been comprehensively analysed during the past (e.g. Türkeş 1998, 1999, 2003, 2013, Türkeş & Tatlı 2009, 2011). Many studies have also revealed that precipitation regime and year-to-year and decadal precipitation variability in Turkey referring to the whole year except summer are associated with the location, variation and activity of the atmospheric disturbances mainly over the North Atlantic and the greater Mediterranean regions (e.g. Türkeş 1998, 2014, Kutiel et al. 2001, Türkeş et al. 2002, Türkeş & Erlat 2003, 2006, Tatlı & Türkeş 2008, Türkeş & Altan 2014). The results of a very recent study performed by Şahin et al. (2015) showed that the displacement of the prevailing atmospheric action centers located over the subtropical mid-east Atlantic (i.e. Azores high-pressure system) and the north-east Atlantic (i.e. Icelandic or mid-latitude frontal low-pressure systems) northward and southward, respectively, determine the predominance of dry and wet conditions over the Mediterranean Basin. In winter, the eddy fluxes originating from the mid-Atlantic propagate over Europe providing wet conditions in the Western and Central Europe, while the contribution of eddies to the moisture budget

weakens in summer months for the Mediterranean Basin, mainly because of weaker and less frequent frontal activity (Şahin et al. 2015). During summer, late spring and early autumn, significant precipitation amounts in Turkey can be associated only with local convective showers and thunderstorms and local orographic rainfall events over mountainous areas with suitable exposure to prevailing humid air flows and/or cyclonic weather systems. Extreme precipitation events in summer are generally less frequent than in winter. The Amonos Mountains parallel to the east coast of the Gulf of Iskenderun, and the Western Taurus Mountains parallel to the Marmaris and Antalya Gulf coasts can be considered as a good example for this type of heavy and extreme orographic rainfall event in Turkey (Türkeş et al. 2016). In this respect, Table 1 displays the extreme rainfall amounts recorded at 3 meteorological stations in Turkey in the standard periods of time. Two of these meteorological stations, Antalya and Marmaris, are located on the western Mediterranean coastal belt of Turkey characterised by a dry and very hot summer subtropical Mediterranean climate (i.e. Csa type of the Köppen-Geiger classification), whereas Hopa station is located on the easternmost coast of the Eastern Black Sea sub-region of Turkey and is characterized by a humid temperate and rainy (in all seasons) climate (i.e. Cfb type of the Köppen-Geiger classification) (Türkeş 2010). The location of these stations are displayed on the map of precipitation regions of Turkey (Türkeş 1998) (Fig. 1). The strongest extreme rainfall event ever recognized in the Mediterranean climate region of Turkey associated with a frontal cyclonic system was attributed to the winter storm of 10–11 November 1992, when 466.3 mm of precipitation were recorded in a 24 h period at the Marmaris meteorological station at the southwest coast (Table 1).

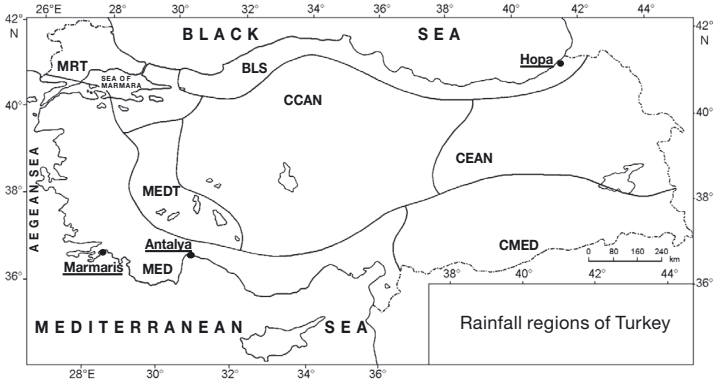

Fig. 1. The precipitation regions of Turkey (Türkeş 1998) along with the location of 3 meteorological stations characterized by extreme precipitation amounts in the standard time periods given in Table 1. Names and abbreviations of the regions: BLS: Black Sea; MRT: Marmara Transition; MED: Mediterranean; MEDT: Mediterranean Transition; CMED: Continental Mediterranean; CCAN: Continental Central Anatolia; and CEAN: Continental Eastern Anatolia

Table 1. Extreme rainfall amounts at the meteorological stations Antalya, Marmaris and Hopa in the standard time periods (see www.mgm.gov.tr/veridegerlendirme/maksimum-yagisalar.aspx#sfU). The locations of these stations are displayed on the map of Turkish precipitation regions (Fig. 1)

Period	Amount (mm)	Location	Date of record (d.mo.yr)
5 min	50.5	Hopa	7.07.1988
10 min	60.6	Hopa	7.07.1988
15 min	70.7	Hopa	7.07.1988
30 min	90.9	Hopa	7.07.1988
1 h	131.0	Antalya	03.11.1995
2 h	180.5	Antalya	04.11.1995
3 h	230.9	Marmaris	11.12.1992
4 h	332.3	Antalya	04.11.1995
5 h	374.3	Antalya	04.11.1995
6 h	390.3	Antalya	05.11.1995
8 h	410.4	Antalya	06.11.1995
12 h	428.1	Antalya	07.11.1995
18 h	464.8	Marmaris	10.–11.11.1992
24 h	466.3	Marmaris	10.–11.11.1992

In the present study, extreme precipitation in Turkey is studied by applying a multivariate statistical methodology scheme involving a data reduction and clustering procedure applied to several atmospheric circulation parameters over the Mediterranean region. This procedure includes the combined use of the multivariate statistical methods factor analysis and cluster analysis. The study aims at the definition and the identification of extreme precipitation events in Turkey and the revelation of the main modes of atmospheric structure over Europe and the Mediterranean that favour their occurrence. The characteristics of atmospheric circulation before, during and after the end of the extreme precipitation events are examined along with their seasonality, duration and spatial distribution.

2. DATA AND METHODOLOGY

The data used in the present study are: (1) Daily precipitation at 70 climatological and synoptic meteorological stations in Turkey (Table 2, Fig. 2a) for the period 1979 to 2011, obtained from the Turkish Meteorological Service (TMS; www.mgm.gov.tr/veridegerlendirme/maksimum-yagisalar.aspx#sfU).

Table 2. The 70 climatological and meteorological stations of Turkey

a/a	Station Name	Latitude (°N)	Longitude (°E)	a/a	Station Name	Latitude (°N)	Longitude (°E)
1	Adana	37.0500	35.3500	36	Kahramanmaraş	37.6000	36.9333
2	Adapazarı	40.7675	30.3933	37	Karaman	37.2000	33.2167
3	Afyonkarahisar	38.7381	30.5606	38	Karapınar	37.7167	33.5333
4	Akhisar	38.9117	27.8233	39	Kars	40.6167	43.1000
5	Amasya	40.6500	35.8500	40	Kayseri	38.7000	35.4833
6	Ankara	39.9725	32.8639	41	Keban	38.8000	38.7500
7	Artvin	41.1833	41.8167	42	Keles	39.9153	29.2311
8	Ayvalık	39.3113	26.6861	43	Kırşehir	39.1636	34.1561
9	Bandırma	40.3314	27.9964	44	Kilis	36.7167	37.0833
10	Bayburt	40.2500	40.2333	45	Konya	37.8686	32.4714
11	Bilecik	40.1414	29.9772	46	Kütahya	39.4172	29.9889
12	Boğazlıyan	39.2000	35.2500	47	Malatya	38.3500	38.2167
13	Bolu	40.7331	31.6025	48	Manavgat	36.7894	31.4411
14	Bursa	40.2308	29.0133	49	Manisa	38.6153	27.4047
15	Ceylanpınar	36.8406	40.0306	50	Merzifon	40.8333	35.4500
16	Çanakkale	40.1411	26.3997	51	Muğla	37.2097	28.3669
17	Çankırı	40.6086	33.6103	52	Muş	38.6833	41.4833
18	Dikili	39.0739	26.8881	53	Ordu	40.9828	37.8989
19	Divriği	39.3667	38.1167	54	Ödemiş	38.2158	27.9642
20	Diyarbakır	37.9000	40.2333	55	Rize	41.0394	40.5111
21	Edirne	41.6767	26.5508	56	Samanda	36.0833	35.9667
22	Edremit	39.5886	27.0528	57	Samsun	41.3436	36.2550
23	Elmalı	36.7372	29.9125	58	Sarıkamı	40.3333	42.5667
24	Erciş	39.3333	43.3500	59	Sarıyer	41.1464	29.0556
25	Erzincan	39.7500	39.5000	60	Siirt	37.9167	42.0000
26	Erzurum	39.9000	41.2833	61	Silifke	36.3833	33.9333
27	Gazipaşa	36.2667	32.3167	62	Sivas	39.7497	37.0208
28	Gemerek	39.1833	36.0667	63	Şanlıurfa	37.1667	38.7833
29	Gökçeada	40.1908	25.9078	64	Şile	41.1686	29.6003
30	Hınıs	39.3667	41.7000	65	Tefenni	37.3161	29.7792
31	Iğdır	39.9167	44.0500	66	Tekirda	40.9586	27.4964
32	Ilgın	38.2833	31.9000	67	Tunceli	39.1167	39.5500
33	İnebolu	41.9789	33.7639	68	Uşak	38.6714	29.4039
34	İspir	40.4833	41.0000	69	Van	38.4667	43.3500
35	İzmir	38.3950	27.2194	70	Zonguldak	41.4492	31.7783

The stations Hopa, Antalya and Marmaris (Table 1) are not included in Table 2, as they are not used in the analysis because of the many missing values in their daily precipitation databases.

(2) 12:00 h UTC ERA-Interim 1° × 1° daily grid point values (Deel et al. 2011) of 500 and 1000 hPa standard pressure level geopotential heights (Z_{500} and Z_{1000}), 500 hPa level relative vorticity (RV), 850 hPa level air temperature (T) and relative humidity (RH), 925 hPa level divergence (DIV) and convective available potential energy (CAPE) for the period 1979 to 2011 over the area defined by the 30° and 50° N parallels and the 10° and 50° E meridians (small domain). For Z_{500}, Z_{1000} and T, a larger domain (25° to 60° N and 10° W to 50° E) is used only for the presentation of the results.

At first, a quantitative approach for examining extreme precipitation in Turkey is followed by defining the following terms:

(1) An extreme precipitation day in Turkey (EPD) is defined as the day with (i) at least 1 climatological/meteorological station characterized by a precipitation amount belonging to the highest 1% percentile of the non-zero daily amounts and (ii) at least 7 stations (10% of the total number) characterized by a precipitation value belonging to the highest 5% percentile. The latter ensures that EPD does not refer to only 1 isolated extreme phenomenon but to at least 1 spatially extended one.

(2) An extreme precipitation event in Turkey (EPE) is defined as a sequence of successive EPDs or a temporally isolated EPD. Thus, an EPE may consist of 1, 2 or more EPDs, and the number of EPDs defines the duration of EPE. An EPE consisting of >1 EPDs may refer to either a persistent/stationary atmospheric disturbance affecting the same region of Turkey for >1 d or a moving atmospheric disturbance affecting different regions of Turkey during its passage across the country.

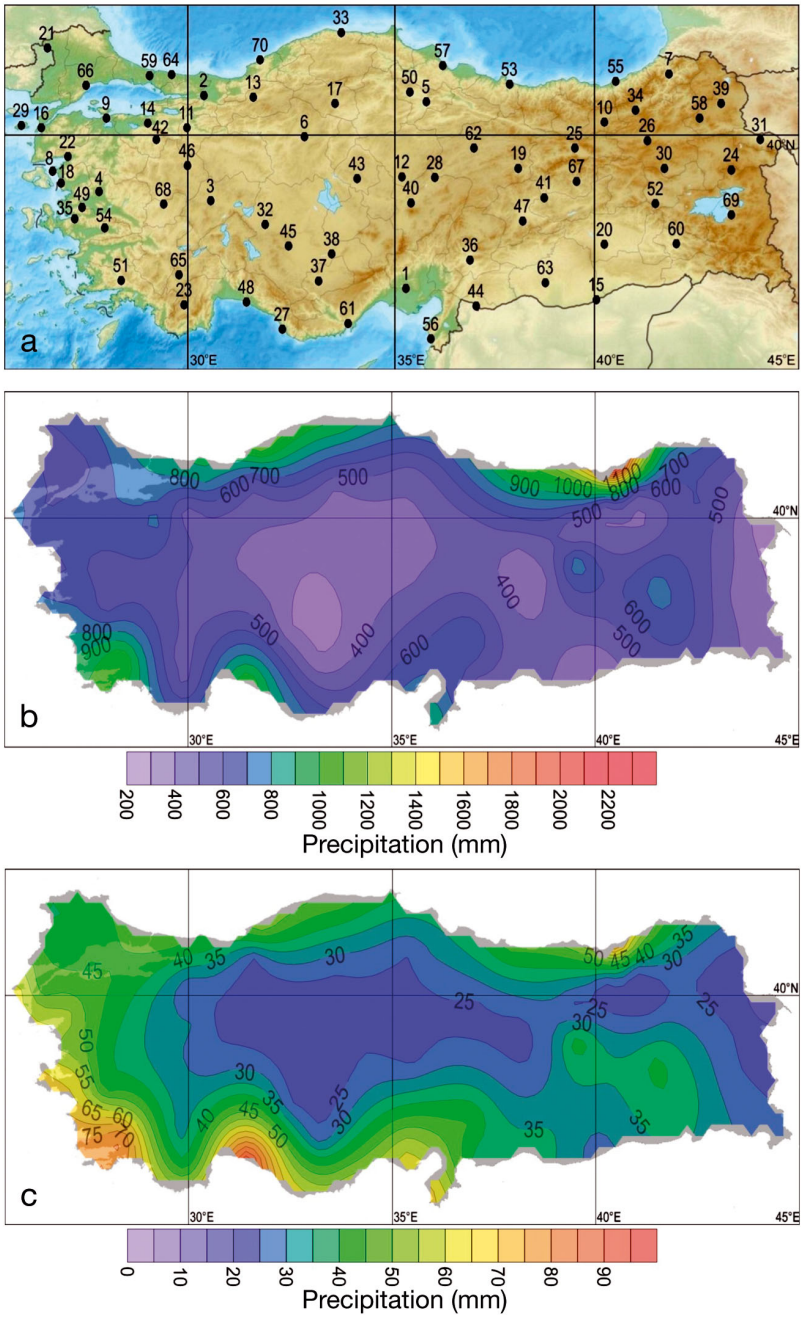

Fig. 2. (a) The geographical locations of the 70 climatological and meteorological stations (numbers correspond to the row numbers of Table 2) and the patterns of (b) the mean annual precipitation (mm) and (c) the top 1% daily precipitation threshold (mm)

Next, a dimensionality reduction process is carried out with the application of *S*-mode factor analysis (FA) with varimax rotation to Z_{500}, Z_{1000} and T for the day before (D–1), the first day (D) and the day following the end (END) of the EPEs found. These 3 days are selected, taking into account that, in general, for an EPE consisting of >1 EPD, the patterns of the atmospheric parameters for the rest of the EPDs (between D and END) resemble the patterns of D day in the case of a stationary atmospheric disturbance, while they present intermediate characteristics between the patterns of D and END days in the case of a moving (usually from west to east) atmospheric disturbance. FA is a dimensionality reduction technique that expresses a group of p variables X_1, X_2, …, X_p in terms of a smaller number of new orthogonal variables in order to reveal the relation between the original p ones (Jolliffe 1986, Manly 1986). Each of the initial p variables can be written as a linear function of the m ($m < p$) new ones (the factors), i.e. $X_i = a_{i1}F_1 + a_{i2}F_2 + \ldots + a_{im}F_m + e_i$, where F_1, F_2, …, F_m are the factors, a_{i1}, a_{i2}, …, a_{im} are the factor loadings which are in fact the correlation coefficients between the initial variables and the factors, and e_i is the specificity that expresses the part of X_i variance not explained by the m factors. FA is a technique similar to empirical orthogonal functions (EOF) and principal component analysis (PCA), which have also been used in climate studies during the last decade (e.g. García-Serrano et al. 2011, Rousi et al. 2015). FA would be essentially equivalent to PCA if the e_i terms in the FA model (the variability not explained by the factors) can be assumed to have the same variance (e.g. Manly 1986). The decision about the number (m) of factors is taken using one of the appropriate statistical tests (Overland & Preisendorfer 1982, Jolliffe 1986). In the present work, SCREE plot is used for the selection of m (Cattell 1952). According to this criterion, m must be the number of points that deviate from a straight line in a plot of the eigenvalues of the correlation matrix of the p initial parameters, ordered from the highest to the lowest one. There are various modes of FA depending on the physical hypostasis of the data matrix lines and columns (e.g. time or space). In the present work, *S*-mode is used. In *S*-mode FA, lines and columns of the data matrix correspond to time and space,

respectively (Richman 1986). The rotation of the axes is a widely used process resulting in better discrimination among the initial variables. There are various types of rotation. In the present work, we use varimax rotation, which keeps the factors uncorrelated (Richman 1986).

In the next step, the EPEs are classified into clusters with characteristic evolution (D−1, D, END) of Z_{500}, Z_{1000} and T patterns, by applying k-means cluster analysis (CA) on the factor scores time series. CA is a clustering technique that classifies observations into objectively defined distinct and homogeneous clusters (Sharma 1995). Decisions about the measure of similarity, the type of clustering procedure (hierarchical or a non-hierarchical) and the number of clusters have to be made. In the case of the present work, the measure of similarity is selected to be the squared Euclidean distance $D_{ij}^2 = \sum_{k=1}^{p} (x_{ik} - x_{jk})^2$, where x_{ik} and x_{jk} are the values of the kth variable for the ith and the jth cases, respectively. The type of clustering procedure is selected to be the k-means technique of the non-hierarchical approach. This technique allows the continuous rearrangement of the observations in new clusters and optimizes the final classification (Davis & Walker 1992, Kalkstein et al. 1996). The decision about the number of clusters is taken using the distortion test introduced by Sugar & James (2003), which is based on the distortion, a quantity that expresses the average distance between the observations and the cluster centres.

The above methodology scheme, i.e. the application of a dimensionality reduction method prior to the clustering process, has been adopted by many researchers in climate studies (see e.g. McGregor & Bamzelis 1995, Lolis 2007). A similar approach to the one of the present work has been followed by Dafis et al. (2016) for snowfall in northwestern Greece. The selection of the circulation parameters has been made taking into account that Z_{500} and Z_{1000} patterns can describe the main circulation characteristics of the middle and the lower troposphere (near the surface) respectively, T and RV patterns provide information about the temperature and humidity characteristics of the lower troposphere significantly connected to precipitation formation (e.g. fronts and low-level cloudiness), RV and DIV are significant parameters related to the upward air movement leading to cloud formation and precipitation, and CAPE expresses the available potential energy in the case of upward air movement connected to the degree of static instability. The analysis includes at the first stages (FA and CA) only Z_{500}, Z_{1000} and T and not the rest of the parameters (RV, RH, etc.) because of their strong dependence on local geographical and relief factors, making their spatial distribution complicated and the data reduction very difficult, with a small amount of variance explained by a large number of components. Alternatively, the mean patterns of these parameters are plotted after the classification procedure along with the patterns of Z_{500}, Z_{1000} and T for each cluster, revealing the general characteristics of their spatial distribution associated with extreme precipitation in Turkey. It is noted that the analysis is applied to Z_{500}, Z_{1000} and T values of the small domain, while the mean patterns of these parameters are presented for the large domain. This selection is made taking into account that although the classification procedure aims to reveal and highlight differences close to the area under study (Turkey), the presented patterns aim at also featuring the main characteristics of the large-scale atmospheric circulation over a broader area over Europe and the Mediterranean.

3. RESULTS AND DISCUSSION

The patterns of the mean annual precipitation and the top 1% daily precipitation threshold are presented in Fig. 2b,c. According to these patterns, high annual amounts exceeding 700 mm are shown over the southwestern and northern areas of Turkey, while high daily top 1% thresholds (above 40 mm) occur along and near the coasts. In contrast, low precipitation amounts and thresholds appear over the continental areas, away from the sea (Fig. 2b,c). According to the definitions of EPD and EPE presented in the previous section, 425 EPDs and 326 EPEs were found for Turkey. The intra-annual and inter-annual variation of EPDs and the duration of EPEs are shown in Fig. 3a–c. EPDs were most frequent during autumn and early winter, with their maximum frequency appearing in November (Fig. 3a). In contrast, very few EPDs were found during the high-summer months July and August. The inter-annual variation of EPDs does not show any statistically significant (95% confidence level) linear trend, while their yearly number ranged from 5 to 20 (Fig. 3b). Also, the duration of most EPEs is 1 d only, and there were no EPEs with duration longer than 4 d (Fig. 3c).

The application of FA on the Z_{500}, Z_{1000} and T grid point data for D−1, D and END days results in 6 factors accounting for 87% of the total variance for each of the 3 days (D−1, D, END), and the application of

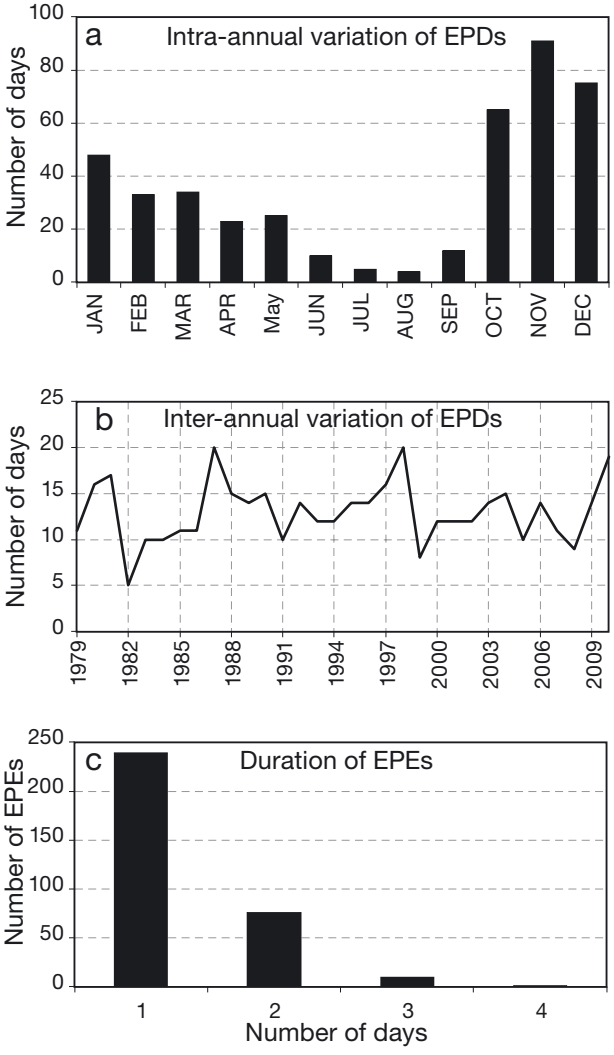

Fig. 3. (a) Inter-monthly and (b) inter-annual variation of the number of extreme precipitation days (EPDs) and (c) duration of extreme precipitation events (EPEs)

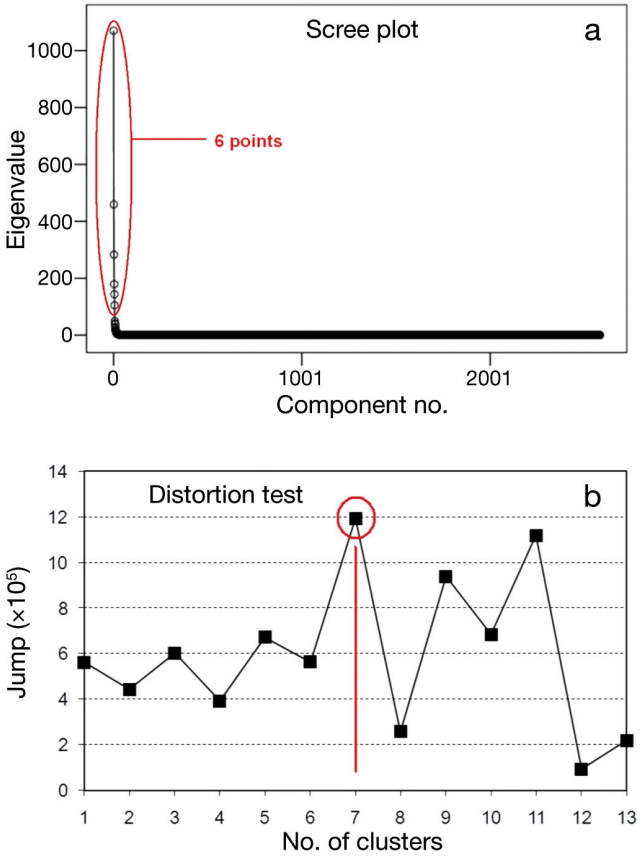

Fig. 4. (a) The Scree plot used for the selection of the number of factors for D day and (b) the 'Jump' plot based on the distortion test used for the selection of the number of clusters. Red markings indicate selected numbers

CA on the 18 (3 days × 6 factors) factor scores time series leads to 7 clusters. As has already been mentioned in the previous section, the number of factors and the number of clusters were selected using a SCREE plot for the D day case (Fig. 4a) and distortion test (Fig. 4b), respectively. According to the SCREE plot, the optimum number of the retained factors is 6, as the number of points clearly deviating from the rest is 6. Similar SCREE plots were found for the other 2 days D–1 and END (not shown). In the distortion test plot, among the cluster numbers ranging between 1 and 13, the highest jump value appears for number 7. Other numbers of factors and clusters were also tested, but according to the physical hypostasis of the results, the above numbers indicated by the 2 tests were the most appropriate. Also, there is no need to examine a higher number of clusters (above 13) because for numbers <13 (e.g. 10, 11, or 12), the differences among the clusters were not recognizable from a physical point of view. For each one of the 7 clusters, the durations of the EPEs are presented in Fig. 5, the intra-annual (month to month) variations of their number are shown in Fig. 6, and the mean EPD precipitation patterns constructed from the station data using Kriging interpolation method appear in Fig. 7. Also, the mean D–1, D and END patterns of Z_{500}, Z_{1000}, T, RV, RH, DIV and CAPE are presented for the 7 clusters in Fig. 8 and Figs. S1–S6 in the Supplement (www.int-res.com/articles/suppl/c071p139_supp.pdf), showing the evolution of atmospheric circulation structure before, in the beginning and after the end of the EPEs. The mean precipitation patterns in Fig. 7 reveal significant differences in the spatial distribution of precipitation among the 7 clusters, although FA and CA have not been applied to precipitation but to atmospheric circulation data. The differences in circulation

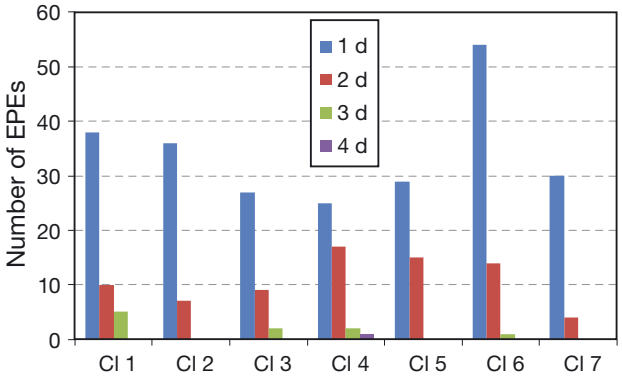

Fig. 5. The duration of the EPEs classified into each of the 7 clusters

associated with the location and the trajectories of the various synoptic disturbances are responsible for different precipitation patterns in Turkey because of the corresponding differences in the areas of upward air movement and the wind direction near the surface. Wind direction is a significant parameter for precipitation formation because it is connected to the humidity of the lower troposphere affected also by the windward or leeward character of the various sub-regions.

Cluster 1 (53 EPEs) is the cluster with the highest number of EPEs lasting for >2 d (5 EPEs). Also, 15 of the 53 EPEs last for >1 d (Fig. 5). Extreme precipitation of Cluster 1 prevails mainly from November to

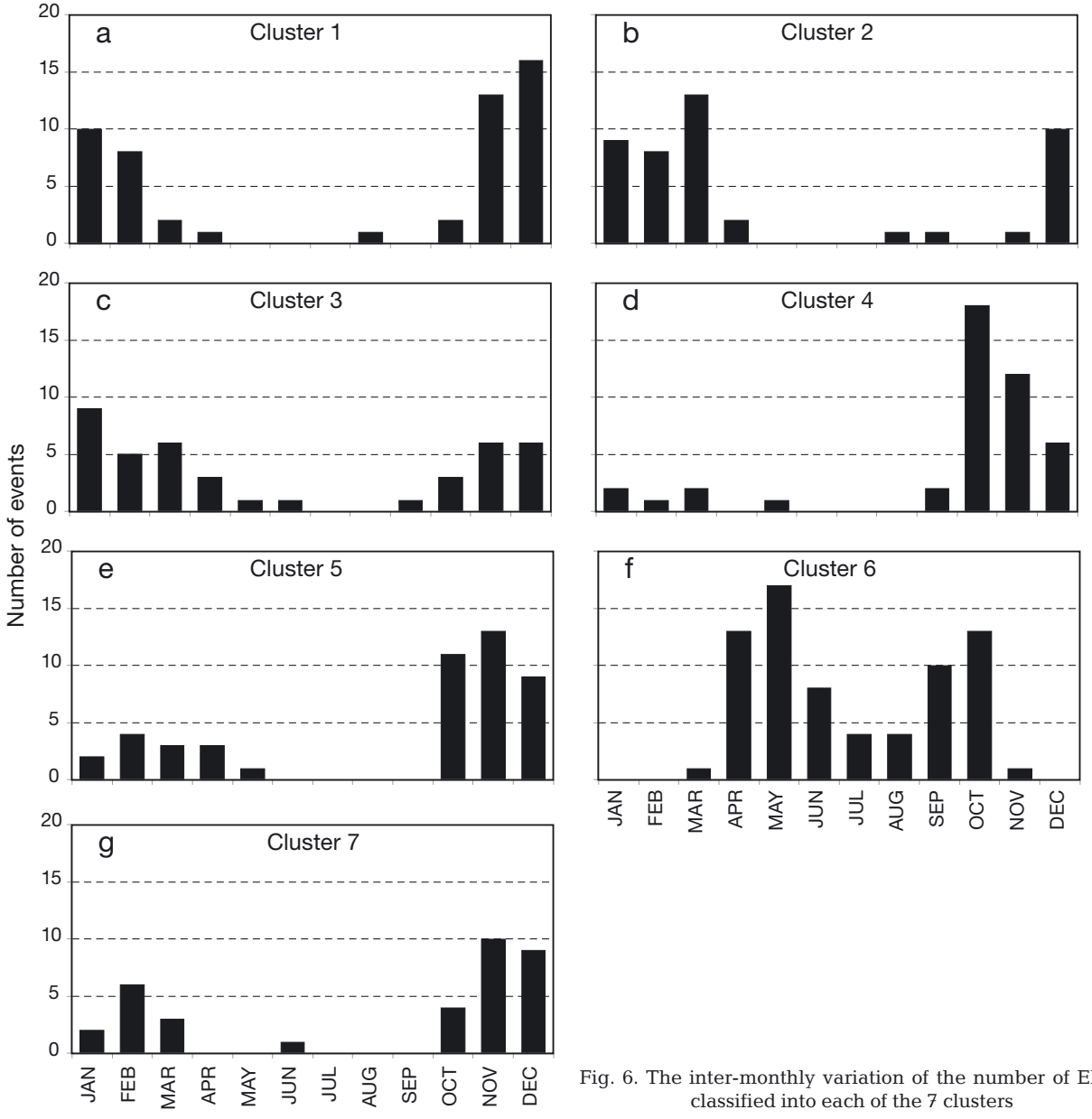

Fig. 6. The inter-monthly variation of the number of EPEs classified into each of the 7 clusters

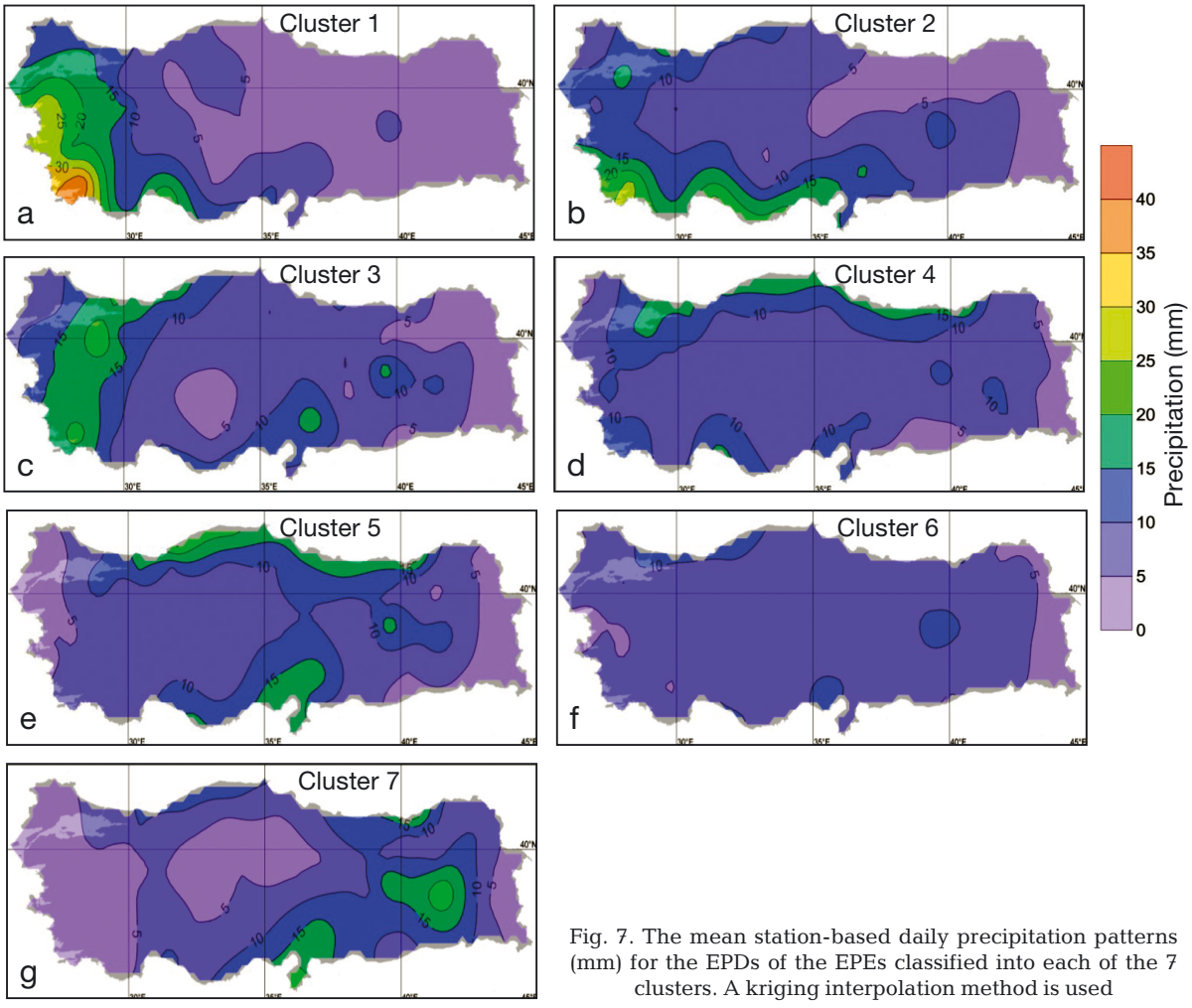

Fig. 7. The mean station-based daily precipitation patterns (mm) for the EPDs of the EPEs classified into each of the 7 clusters. A kriging interpolation method is used

February, while its maximum frequency appears in December (Fig. 6a), when the mid-latitude cyclones originating over the northeast Atlantic and the frontal low-pressure systems originating over the Mediterranean become most frequent and intense (Türkeş 1998, 2010). Mean daily precipitation peaks over southwest Anatolia, exceeding 35 mm (Fig. 7a). The mean patterns of the atmospheric parameters during D–1, D and END days are shown in Fig. 8. According to Fig. 8, the EPEs classified in Cluster 1 are connected to a west to east moving atmospheric disturbance causing significant positive vorticity advection, low level convergence and high instability and humidity levels over the western and especially the south-western part of the country. During D–1 day, a large-scale trough at the 500 hPa level covering central Europe and the central Mediterranean, and a surface low-pressure system over the mid-northern Mediterranean basin, the Aegean Sea and the Balkans are shown, causing warm advection over the south-eastern Aegean and high convergence (negative DIV values), relative humidity and CAPE values along the western coasts of Turkey. The surface flow over the western coasts of Turkey is south-westerly transferring very humid surface air masses from the central Mediterranean and the Aegean Sea. On D day, the 500 hPa level trough axis is over the Aegean Sea and the Balkans with the maximum vorticity values over the south-eastern Aegean and the south-western Anatolia regions, while the surface low-pressure system presents 2 centres, the first one over the Black Sea and the second one over the Aegean Sea and western Anatolia. The area of warm advection moves slightly eastward, while high convergence and RH zones appear over the high-precipitation area of southwest Turkey. On END day, the main disturbance moves eastwards and weakens, while another one appears over the Adriatic Sea. Convergence, RH and CAPE decrease over the area of high precipitation, favouring the end of the event.

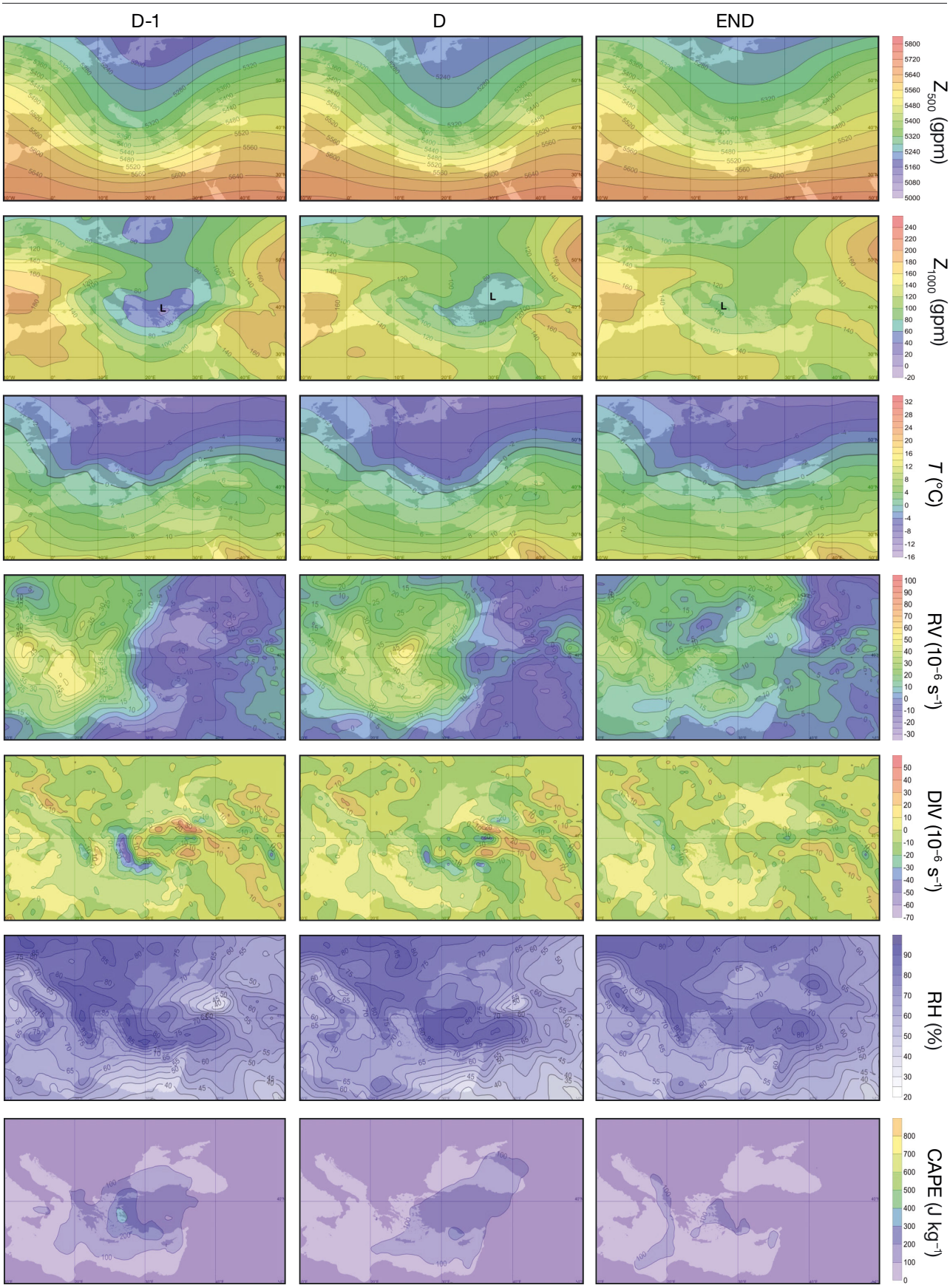

Fig 8. The mean patterns of 500 hPa and 1000 hPa geopotential heights (Z_{500} and Z_{1000}), 500 hPa relative vorticity (RV), 850 hPa air temperature (T) and relative humidity (RH), 925 hPa divergence (DIV) and convective available potential energy (CAPE) for the day before (D–1), the first day (D) and the day following the end (END) of the EPEs found for Cluster 1. A kriging interpolation method is used

Cluster 2 (43 EPEs) is generally characterized by short duration (Fig. 5). It is frequent during the cold period of the year, and its maximum frequency is shown in March (Fig. 6b). Daily precipitation is high mainly along the southern coasts of the country, where both frontal and orographic clouds and rainfall dominate (Fig. 7b). According to the mean patterns of synoptic-scale weather conditions related with the atmospheric parameters during D−1, D and END days (Fig. S1), a well-organized atmospheric disturbance over the southern Balkans moves from west to east affecting southern Turkey. The southern displacement of the trajectories of the low-pressure centre and the positive vorticity, convergence and instability maxima relative to the ones of Cluster 1 justify the corresponding displacement of the high-precipitation zone from the western−southwestern to the southern areas of Turkey. On D−1 day, the depression is located over the southern Aegean Sea, the mid-northern Mediterranean basin and the south-western Anatolia region, and on D day, it moves eastward affecting mainly the southern regions of the country. The positive vorticity center over the southern Aegean is also intensified and moves eastward, while cold advection is shown over the same area. RH and CAPE values are high, while a convergence zone (negative DIV values) appears mainly along the Mediterranean coasts of Turkey. An EPE ends when the whole system and the corresponding positive vorticity and convergence areas weaken and move eastward toward the Middle East. RH values remain relatively high over the eastern part of the country and may be responsible for the retention of lower surface temperatures, stratiform clouds and weak to moderate precipitation there.

Cluster 3 (38 EPEs) can also be characterized as a cold period cluster (Fig. 6c). The corresponding EPEs last mainly for 1 d (27 EPEs), while this cluster also contains 9 and 2 EPEs that last for 2 and 3 d, respectively (Fig. 5). Precipitation is generally high over the west of the country, with a zone of >20 mm appearing in western Anatolia (Fig. 7c). According to the synoptic-scale patterns of atmospheric parameters (Fig. S2), a west to east moving atmospheric disturbance associated with the westerly upper air flow that affects the whole country is evident. The surface low-pressure system with an evident surface trough toward the central Mediterranean covers the Aegean Sea, the mid-northern Mediterranean basin, the west Black Sea and north-west Turkey on D−1 day and the central Anatolia, the central Black Sea and the Mediterranean regions of Turkey on D day. Positive vorticity is transferred mainly along the southern coasts, while convergence is highest over the western part of the country during D−1 day, and presents positive values (negative DIV values) over most of the country on D day. RH is high during both D−1 and END days, exceeding 80% over a large area. CAPE is high over the whole country on D−1 day, while on D day, high values are confined mainly over the eastern part. EPE ends due to the eastward movement and weakening of the upper air and surface systems during END day, while convergence, RH and CAPE values decrease significantly.

Cluster 4 (45 EPEs) is an autumn one as the corresponding EPEs appear mainly in October and November (Fig. 6d). Most EPEs last for 1 or 2 d, while there are 2 EPEs that last for 3 d and only 1 EPE that lasts for 4 d (Fig. 5). The EPEs of Cluster 4 are associated with a generally westerly upper air flow at the eastern side of an upper level trough prevailing over the regions of Eastern Europe, the Balkans and the Aegean Sea, as was generally the case for the previous clusters, but in this case, the areas of Turkey that are mostly affected are the northern ones (Fig. 7d, see Fig. S3 in the supplement). This pattern is due to the fact that the surface flow over the region is north-easterly, causing orographic rainfall superimposed on frontal rainfall, and the associated high humidity zone is over the northern windward parts of Turkey, particularly along the Black Sea coasts (e.g. Türkeş 1998, Kutiel et al. 2001, Türkeş et al. 2002, Türkeş & Erlat 2006), where a humid-temperate climate and rainfall regime prevail (Türkeş 2010, Iyigün et al. 2013). Specifically, atmospheric circulation during D−1 day is characterized by the presence of a widespread high-pressure system over Europe and a depression over the south-eastern Aegean and the south-western coasts of Turkey. Both systems move eastward during D day, forming a north-easterly flow over almost the whole country except the south-eastern Anatolia region, enhancing the baroclinicity, especially along the northern coasts. A high CAPE zone appears over Turkey moving eastward, but the highest values are shown over the Eastern Mediterranean basin, east of Cyprus. On END day, the depression weakens, as do the pressure gradient and the corresponding north-easterly flow over Turkey. High RH values still appear over the north-eastern part of the country, which may be responsible for stratiform cloudiness and weak to moderate precipitation there.

Cluster 5 (44 EPEs) comprises EPEs that appear from October to May, and their maximum frequency is in November (Fig. 6e). The duration of the EPEs is 1 or 2 d, and in this case, there are no EPEs with dura-

tion >2 d (Fig. 5). The areas of Turkey that are mostly affected are the northern coasts, but high precipitation is also shown over the south-central parts of the country (Fig. 7e). The synoptic-scale atmospheric conditions associated with the EPEs of Cluster 5 show a west to east movement of an upper atmospheric trough at the 500 hPa standard pressure level along with a cold front (Fig. S4). The strong north-easterly flow and the negative air temperatures associated with the cold advection appearing on D day imply that the precipitation form in the northern parts of the country may be snow, at least in the high-altitude areas. Positive vorticity advection is very high over almost the whole country, while there is a very high relative humidity zone moving eastward along the northern coasts between D–1 and D days. Convergence is also shown over most areas for both D–1 and D days, while a high CAPE area moves across the country from D–1 to D day. The existence of the high-precipitation zone over south-central Turkey appearing in Fig. 7e can be attributed mainly to dynamic factors and specifically to the fact that this area is very close to the maxima of positive vorticity and convergence. The EPE ends when the upper air trough moves eastward, the north-easterly flow over Turkey weakens, and convergence, relative humidity, vorticity and instability values decrease significantly. Clusters 4 and 5 are the clusters with the highest percentage of EPEs lasting for >1 d. This is possibly due to the fact that in both clusters, orography plays an important role in precipitation of the northern areas, even when the magnitude of the main dynamic factors has been reduced (e.g. on the second day of the EPEs). The very cold air masses passing over the relatively warm surface of the Black Sea may cause significant amounts of orographic precipitation in the northern windward areas, taking advantage of the high vertical temperature and relative humidity gradients in the lowest tropospheric layers and the associated high convective instability.

Cluster 6 (69 EPEs) can be characterized as the warm period cluster, as the corresponding EPEs appear mainly from April to October (Fig. 6f). In this cluster, 54 of 69 EPEs last for 1 d, 14 of them last for 2 d, only 1 of them last for 3 d, and there are no EPEs with duration longer than 3 d (Fig 5). Mean daily precipitation is relatively evenly distributed over the whole country, not presenting any remarkable spatial maxima or minima (Fig. 7f). The atmospheric circulation characteristics favouring the EPEs of Cluster 6 are presented in Fig. S5, revealing the typical synoptic conditions being responsible for extreme precipitation during the warm period of the year in the Mediterranean. The Z_{1000} patterns are similar to the corresponding climatic patterns of the warm period of the year, characterized by the presence of the thermal low associated with the western and north-western (mainly surface-based) extension of the South Asia monsoonal low and the anticyclonic conditions over Europe and the western and central Mediterranean (e.g. Türkeş & Erlat 2006, Lolis et al. 2008, Erlat & Türkeş 2013, Şahin et al. 2015, etc.). The Z_{500} patterns show a west to east movement of a trough over the Eastern Mediterranean affecting the whole country. On D–1 day, a spatially extended vorticity maximum covers the southern Balkans, Western Turkey and the Eastern Mediterranean Sea, centred over the southwest coasts of Turkey. This maximum moves eastward during D day, covering the whole country and centred over the Cyprus region. The upper air trough and the intense land warming prevailing during the warm period of the year favour instability conditions appearing in CAPE patterns, especially on D–1 day over the eastern part of the country. Finally, low-level convergence and high relative humidity values prevail mainly on D–1 and D days, especially over the northern part of the country. The EPEs end with the weakening and the eastward movement of the upper air disturbance and the associated decrease of static instability. It has to be noted that Cluster 6 represents warm season events, but the filtering process of EPEs does not allow for mesoscale convective events (those that either occur on a sub-daily scale or are not widespread). Such mesoscale events are probably associated with atmospheric circulation characteristics similar to those of Cluster 6, taking into account that the combination of the upper air trough shown in Fig. S5 and the intense land warming can be responsible for mesoscale convective events during the warm season, especially over the continental and mountainous regions.

Cluster 7 (34 EPEs) is another cluster of the cold period, as all the corresponding EPEs appear during the period October to March, except one of them which appears in June (Fig. 6g). Thirty of the 34 EPEs last for 1 d only, while the rest of them last for 2 d (Fig. 5). The precipitation pattern of Cluster 7 shows that the highest amounts appear over the Eastern Mediterranean sub-region and the south-eastern Anatolia region, with daily values exceeding 20 mm over a small mountainous district (east segment of the south-eastern Taurus Mountains) (Fig. 7g). The synoptic conditions associated with Cluster 7 show a deep upper air trough with a strong geopotential height gradient over Turkey during D–1 day and an

upper air low formed during D day, while in the lower troposphere, the Turkish area is under the influence of the combination between an anticyclone centred over the Balkans and a low-pressure system over the Cyprus, Syria and south-eastern Anatolia regions (Fig. S6). This combination is responsible for the north-easterly flow and the associated cold advection leading to negative 850 hPa pressure level air temperatures over the northern part of the country. Relative vorticity increases significantly over the south-eastern part of the country, where instability is high because of the presence of the upper low-pressure system centre and the associated cold air mass, low level convergence prevails, and the highest daily precipitation amounts are shown. The EPEs end with the eastward displacement and the weakening of the disturbance leading to corresponding changes to all the significant atmospheric parameters over the region.

4. CONCLUSIONS

Extreme precipitation in Turkey and the associated atmospheric circulation characteristics are examined, and the results lead to the following conclusions:

(1) According to the intra-annual variation of the number of extreme precipitation events, these events are mainly concentrated during late autumn and early winter, while only a few events appear during the warm period of the year from June to September.

(2) According to the inter-annual variation of the number of the events, there is no statistically significant trend of their number during the period under study.

(3) The duration of the events is relatively short with most of the events lasting for 1 d only, while there is no event with duration longer than 4 d.

(4) The application of FA and CA on atmospheric circulation data led to 7 modes of atmospheric circulation evolution favouring the occurrence of extreme precipitation in Turkey. According to the general features of these modes, the synoptic conditions that favour the occurrence of the events are characterized mainly by the west to east movement of strong large-scale upper atmospheric troughs and deep surface low-pressure systems associated with significant positive vorticity advection, high relative humidity over the lower troposphere, and convergence and high instability zones over specific sub-regions of the country. In most cases of extreme events, the presence of a surface low-pressure system over the Eastern Mediterranean basin south of Turkey, particularly over the Cyprus region, is one of the dominant characteristics of the prevailing atmospheric circulation.

(5) It has been found that 6 of the 7 modes of circulation evolution prevail mainly during the cold period of the year, while only 1 mode prevails during the warm period. Considering the 6 clusters of the cold period, 3 of them refer to the eastern/south-western part of the country, 2 of them refer mainly to the northern coastal areas, and 1 of them corresponds to the eastern continental area. The differences among the precipitation patterns can be attributed to the locations and the trajectories of the vorticity, convergence, humidity and instability maxima and the effect of orographic lifting depending on the surface flow direction. The warm period cluster is characterized by a relatively uniform precipitation pattern because precipitation is mainly a result of convection due to the land warming and high static instability, which are relatively uniform over the country when cold upper air masses dominate over a large area.

(6) Finally, the Mediterranean depressions play the most important role in the occurrence of extreme precipitation events during the cold period of the year. In contrast, in summer, low upper air temperatures and high static instability associated with the land warming and the presence of upper air disturbances are the main causes.

The results of the present work reveal the subregions of Turkey that are mostly affected by specific evolution types of atmospheric circulation patterns, and therefore, these results can be useful for extreme precipitation forecasting in Turkey. The forecaster can take into account these results along with the outputs of the numerical models, because the forecast uncertainty based on the unavoidable uncertainty of the numerical model outputs can be partly reduced by using a statistical tool based on real extreme precipitation data over a long time period.

LITERATURE CITED

Cattell RB (1952) Factor analysis. Harper, New York, NY

Dafis S, Lolis CJ, Houssos EE, Bartzokas A (2016) The atmospheric circulation characteristics favoring snowfall in an area with complex relief in Northwestern Greece. Int J Climatol 36:3561–3577, doi:10.1002/joc.4576

Davis RE, Walker DR (1992) An upper air synoptic climatology of the western United States. J Clim 5:1449–1467

Dayan U, Nissen K, Ulbrich U (2015) Review Article: Atmospheric conditions inducing extreme precipitation over the eastern and western Mediterranean. Nat Hazards Earth Syst Sci 15:2525–2544

Deel DP, Uppala SM, Simmons AJ, Berrisford P and others (2011) The ERA-Interim reanalysis: configuration and performance of the data assimilation system. QJR Meteorol Soc 137:553–597

Erlat E, Türkeş M (2013) Observed changes and trends in numbers of summer and tropical days, and the 2010 hot summer in Turkey. Int J Climatol 33:1898–1908

Flaounas E, Drobinski P, Vrac M, Bastin S and others (2013) Precipitation and temperature space-time variability and extremes in the Mediterranean region: evaluation of dynamical and statistical downscaling methods. Clim Dyn 40:2687–2705

García-Serrano J, Rodríguez-Fonseca B, Bladé I, Zurita-Gotor P, de la Cámara A (2011) Rotational atmospheric circulation during North Atlantic-European winter: the influence of ENSO. Clim Dyn 37:1727–1743

Houssos EE, Lolis CJ, Bartzokas A (2008) Atmospheric circulation patterns associated with extreme precipitation amounts in Greece. Adv Geosci 17:5–11

Iyigün C, Türkeş M, Batmaz İ, Yozgatlıgil C, Gazi VP, Koç EK, Öztürk MZ (2013) Clustering current climate regions of Turkey by using a multivariate statistical method. Theor Appl Climatol 114:95–106

Jolliffe IT (1986) Principal component analysis. Springer, New York, NY

Kalkstein LS, Nichols MC, Barthel CD, Greene JS (1996) A new spatial synoptic classification: application to air mass analysis. Int J Climatol 16:983–1004

Krichak SO, Breitgand JS, Gualdi S, Feldstein SB (2014a) Teleconnection-extreme precipitation relationships over the Mediterranean region. Theor Appl Climatol 117: 679–692

Krichak SO, Barkan J, Breitgand JS, Gualdi S, Feldstein SB (2014b) The role of the export of tropical moisture into midlatitudes for extreme precipitation events in the Mediterranean region. Theor Appl Climatol 121: 499–515

Kutiel H, Hirsch-Eshkol TR, Türkeş M (2001) Sea level pressure patterns associated with dry or wet monthly rainfall conditions in Turkey. Theor Appl Climatol 69:39–67

Lolis CJ (2007) Climatic features of atmospheric stability in the Mediterranean region (1948-2006): spatial modes, inter-monthly and inter-annual variability. Meteorol Appl 14:361–379

Lolis CJ, Metaxas DA, Bartzokas A (2008) On the intra-annual variability of atmospheric circulation in the Mediterranean region. Int J Climatol 28:1339–1355

Lolis CJ, Bartzokas A, Lagouvardos K, Metaxas DA (2012) Intra-annual variation of atmospheric static stability in the Mediterranean region: a 60-year climatology. Theor Appl Climatol 110:245–261

Manly BFJ (1986) Multivariate statistical methods: a primer. Chapman & Hall, London

McGregor GR, Bamzelis D (1995) Synoptic typing and its application to the investigation of weather air pollution relationships, Birmingham, United Kingdom. Theor Appl Climatol 51:223–236

Nastos PT, Kapsomenakis J, Douvis KC (2013) Analysis of precipitation extremes based on satellite and high-resolution gridded data set over Mediterranean basin. Atmos Res 131:46–59

Overland JE, Preisendorfer RW (1982) A significance test for principal components applied to a cyclone climatology. Mon Weather Rev 110:1–4

Parker LE, Abatzoglou JT (2016) Spatial coherence of extreme precipitation events in the Northwestern United States. Int J Climatol 36:2451–2460

Pfahl S, Wernli H (2012) Quantifying the relevance of cyclones for precipitation extremes. J Clim 25:6770–6780

Richman MB (1986) Rotation of principal components. J Climatol 6:293–335

Rousi E, Anagnostopoulou C, Tolika K, Maheras P (2015) Representing teleconnection patterns over Europe: a comparison of SOM and PCA methods. Atmos Res 152: 123–137

Şahin S, Türkeş M, Wang SH, Hannah D, Eastwood W (2015) Large scale moisture flux characteristics of the Mediterranean basin and their relationships with drier and wetter climate conditions. Clim Dyn 45:3381–3401

Sharma S (1995) Applied multivariate techniques. Wiley, New York, NY

Sugar AC, James MG (2003) Finding the number of clusters in a dataset: an information — theoretic approach. J Am Stat Assoc 98:750–763

Tatlı H, Türkeş M (2008) Drought events of 2006/2007 in Turkey and determination of its association with large-scale atmospheric variables by logistic regression. In: 5th Atmos Sci Symp Proc, İstanbul, p 516–527 (in Turkish)

Toreti A, Giannakaki P, Martius O (2016) Precipitation extremes in the Mediterranean region and associated upper-level synoptic-scale flow structures. Clim Dyn 47: 1925–1941

Türkeş M (1998) Influence of geopotential heights, cyclone frequency and Southern Oscillation on rainfall variations in Turkey. Int J Climatol 18:649–680

Türkeş M (1999) Vulnerability of Turkey to desertification with respect to precipitation and aridity conditions. Turk J Eng Environ Sci 23:363–380

Türkeş M (2003) Spatial and temporal variations in precipitation and aridity index series of Turkey. In: Bolle HJ (ed) Mediterranean climate — variability and trends. Regional climate studies, Springer Verlag, Heidelberg, p 181–213

Türkeş M (2010) Climatology and meteorology, 1st edn. Publication No. 63, Physical Geography Series No. 1, Kriter Publisher, İstanbul (in Turkish)

Türkeş M (2013) Observed and projected climate change, drought and desertification in Turkey. Ankara Univ J Environ Sci 4:1–32 (Ankara Üniversitesi Çevre Bilimleri Dergisi)

Türkeş M (2014) Analysis of 2013-2014 drought in Turkey and its climatological and meteorological reasons. Konya Soil Water J 2:20–34 (Konya Toprak Su Dergisi)

Türkeş M, Altan G (2014) Climatological analysis of forest fires occurred in 2011 over Turkey and their associations with hydroclimatic, surface weather and upper atmosphere conditions. Int J Hum Sci 11:145–176 (in Turkish with English abstract and summary)

Türkeş M, Erlat E (2003) Precipitation changes and variability in Turkey linked to the North Atlantic Oscillation during the period 1930-2000. Int J Climatol 23:1771–1796

Türkeş M, Erlat E (2006) Influences of the North Atlantic Oscillation on precipitation variability and changes in Turkey. Nuovo Cimento Soc Ital Fis C 29:117–135

Türkeş M, Tatlı H (2009) Use of the standardized precipitation index (SPI) and modified SPI for shaping the drought probabilities over Turkey. Int J Climatol 29:2270–2282

Türkeş M, Tatlı H (2011) Use of the spectral clustering to determine coherent precipitation regions in Turkey for the period 1929-2007. Int J Climatol 31:2055–2067

Türkeş M, Sümer UM, Kılıç G (2002) Persistence and periodicity in the precipitation series of Turkey and associa-

tions with 500 hPa geopotential heights. Clim Res 21: 59–81

Türkeş M, Musaoğlu N, Erten E, Özcan O (National Consultants) (2016) Vulnerability assessment to climate change and variability of the Mediterranean forest ecosystem in the pilot site of Düzlerçamı, Turkey. 'Maximize the production of goods and services of Mediterranean forest ecosystems in the context of global changes (GCP/GLO/458/FRA)', Component 1 'Production of data and development of tools to support decision and management of vulnerable Mediterranean forest ecosystems affected by climate change and the ability of these forest ecosystems to adapt to global change'. January 2016 (Project Report), FAO, Silva Mediterranea, FFEM, OGM. (In press)

Winschall A, Sodemann H, Pfahl S, Wernli H (2014) How important is intensified evaporation for Mediterranean precipitation extremes? J Geophys Res Atmos 119:5240–5256

Editorial responsibility: Oliver Frauenfeld, College Station, Texas, USA

Submitted: March 29, 2016; Accepted: September 22, 2016
Proofs received from author(s): December 3, 2016